

Comparison of Simulation and Experiment Results of Oil Film Temperature of the Connecting-Rod Big End Bearing in the Experimental Device

Trung Thien Pham¹, Thi Thanh Hai Tran^{2*}, Trong Thuan Luu²

¹University of Economics - Technology for Industries

²Hanoi University of Science and Technology - No. 1, Dai Co Viet Road, Hanoi, Vietnam

Received: March 29, 2020; Accepted: June 22, 2020

Abstract

The paper compares the simulation and experiment results of the lubricating oil temperature in the connecting-rod big end bearing. Simulating hydrodynamic lubrication for the connecting-rod big end bearing based on solving Reynolds equations, oil film thickness equations, load balancing equations and energy equations combined numerical lubrication simulation for the bearing by modeling thermal problems for oil films using finite element method. Experimental device and simulated rod made of elastic optical material are under the same load as that of a four-stroke engine. The temperature is measured by six thermocouple sensors located at positions 0° , 45° , 135° , 180° , 225° , 315° of the connecting-rod and at the middle section of the bearing along the length direction. The results from the research show the similarity between the simulation result and experience result. The temperature of the oil film in the connecting-rod big end bearing increases when the rotation speed increases and reaches the maximum value at the middle section of 360° angle of the crankshaft when there is an explosion. The higher viscosity the lubrication oil has, the higher temperature of the oil film it is in the connecting-rod big end bearing.

Keywords: Oil film temperature, connecting rod, lubrication.

1. Introduction

The lubrication for the connecting-rod big end bearing is particularly important because it determines the performance and engine lifespan. The study of lubrication for the connecting-rod big end bearing is divided into two main areas: theoretical and experimental researches.

The simulations of hydrodynamic or elastic hydrodynamic lubrication studies use numerical methods such as finite element method or finite difference method to calculate the simulation. Since 1969, scientists around the world have started using numerical methods to solve lubrication problems with bearings under static load. Typically in 1969, Reddy et al. [1] were the first to introduce finite element method in lubrication studies. In 1973, OH and Huebrer [2] first calculated the deformation of the structure. The authors used the finite element method to solve the Reynolds equation with elastic and liquid equations with the isoviscous assumption. The author has expressed the force $\{F\}$ as function $\{\sigma\}$ by the stiffness matrix $[K]$. The knot forces are determined by integrating the pressure field ignoring negative pressure. The study used the Newton-Rapson method

to determine and then inversed the Jacobin matrix [J]. However, this method is limited by the long calculation time. Moreover, the iteration diagram for the problem of fast divergence when the deformation of the surface is large compared to the radius gap. In 2015, H. Shahmohamadi et al [3] study the thermal effects in big end bearing lubrication. They studied flow equation with hydrodynamic effect combining Navier-Stokes solution for flow equation and energy equation. The study offered a solution to simulate fluid flow. In 2018, N. Morris [4] et al. studied the effect of shaft and housing bearing failures in the big end bearing in operation, yielded generated damage and reduced performance until totally destroyed. Experimental research on connecting-rod big end bearing lubrication is divided into two research areas: simulated transmission research and real transmission research.

In 1983, Pierre-Eugene [5] and colleagues investigated the elastic deformation of a big end bearing under the effect of a static load. The rod is cast from epoxy resin. To make the measurements, the authors used optical methods, especially the laser spot method. Connecting-rod is fitted with steel shaft, rotating shaft with speed of 50 to 200 rpm, the load effect varies from 60N to 300N. In 2001, Moreau [6] measured the oil film thickness of the three crankshaft bearings and the large drive shafts of four-

*Corresponding author: Tel.: (+84) 978263926
Email: hai.tranthithanh@hust.edu.vn

cylinder gasoline engines. The author studies the effect of lubricant viscosity, radius gap to oil film thickness. The measurement results are compared with numerical calculation results and give compatible results. In 2005, Michaud [7] and Fatu [8] participated in the construction of the Megapascal test tape to study lubricating the large end drive in real and harsh working conditions. The maximum engine speed reaches 20,000 rpm with compressive and tensile loading of 90 KN and 60 KN. In 2015, M'hammed El Gadari, Aurelian Fatu, Mohamed Hajjam [9] studied simulation and experimental hydrodynamic effect on hydrodynamic bearings. The study shows the influence of bending force on oil film thickness and produces elastic hydrodynamic effect on elastic surface.

In this paper, authors compare the simulation study results and the experimental results of lubricating oil film temperature in the connecting-rod big end bearing.

2. Experimental device.

The experimental device for lubricating the connecting-rod big end bearing is designed with crankshaft mechanism in which the connecting-rod movement follows the principle of the crankshaft system and is subjected to cyclic loading effect of the engine. Experimental equipment has the principle diagram as shown in Figure 1. The electric motor (2) rotates giving the motion to the crankshaft (11) via the reducer, causing the crankshaft to rotate, when the crankshaft pulls the piston guide (5) up and down movement by being connected through the rod. Steel transmission with shaft, small end with piston guide. This assembles along the two pillars of the frame, connecting (the pillar) between the piston guide and the small end of the transmission and shaft, as well as between the transmission rod and the crankshaft thanks to the bearing. In the working process, the transmission rod (edge) in turn pushes the piston upwards and pulls down, this movement follows the margin-crank system of the heat engine. Piston (7) is linked to the crankshaft (11) transmits motion down the shaft of the research bearing (10) fitted with the crankshaft via the research of the connecting-rod (9a + 9b) simulating the piston work in the engine. The connecting-rod for research has two parts, a small end (9a) made of steel and a large end (9b) made of PLM4 epoxy resin and PLMH4 additives. The connecting-rod in this research is placed in parallel with the transmission rod. The connecting-rod big end bearing includes the rod body, connecting-rod and crankshaft. The small end of the research rod links and slides under the piston. In operation (when the shaft rotates), the forces generated by the piston movement and the rod are balanced by the pressure in

the connecting-rod oil diagram. In order to ensure the simulation of the explosion more precise as in the real engine, such as the 4 stroke engine, the piston guide is connected to a generating-load mechanism acting on the piston (7), the camshaft (6) is driven by pulleys and straps (4).

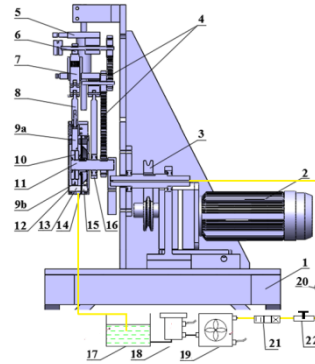


Fig. 1. Principle diagram of experimental device

The sensor consists of two different metal wires, chemically welded together, on one end (hot end) and the other (cold end).

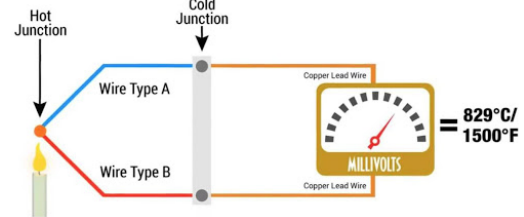


Fig. 2. Structure of thermocouple sensor

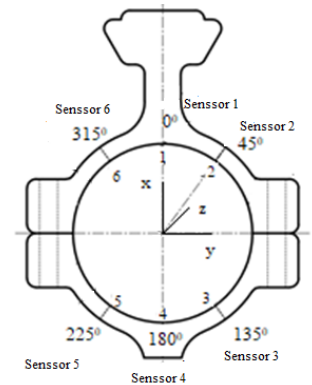


Fig. 3. Sensor Location

Based on the difference in temperature between the two leads of those two wires (hot and cold ends), an electromotive force in the circuit appears. By the measurement of electromotive force, we can obtain the corresponding temperature. Oil temperature of big end bearing is measured at six typical locations in the circumference direction and in the middle section of the drive in the length direction (Figure 3) by six temperature sensors. The sensor will be connected to

the module of the data processor and programmed temperature measurement by LabView software. The sensors are located at locations 0° , 45° , 135° , 180° , 225° , 315° in the circumference of the connecting-rod big end bearing. At the same time, the sensors are also placed on the connecting-rod in the middle section of the bearing along the length direction.

The program for measuring the oil film temperature of the connecting-rod big end bearing following the algorithm diagram. Sampling time is determined from the rotation speed of the engine when tested. The measurement results are displayed on the software interface and saved in the data file. The sensor continuously sends analog signals to the DAQ signal processor, the signal processor converts from the digital signal anal (ADC) signal, the digital signal is transferred to the data logger, when it is the time to sample, the graphical interface will display the measured temperature of the six sensors. The measurement signals of the six sensors are processed simultaneously and the measurement results are recorded in the data file.

3. Simulate oil film temperature field.

The general energy equation in the Oxyz coordinate system is written for the lubricant membrane:

$$\begin{aligned} \delta C_p \left(u \frac{\partial T}{\partial x} + v \frac{\partial T}{\partial y} + w \frac{\partial T}{\partial z} \right) \\ = \frac{\partial}{\partial x} \left(k \frac{\partial T}{\partial x} \right) + \frac{\partial}{\partial y} \left(k \frac{\partial T}{\partial y} \right) + \frac{\partial}{\partial z} \left(k \frac{\partial T}{\partial z} \right) + \mu \left[\left(\frac{\partial u}{\partial y} \right)^2 + \left(\frac{\partial w}{\partial y} \right)^2 \right] \end{aligned} \quad (1)$$

C_p is specific heat capacity; u , v , w are velocities in the x , y , z directions; k is the heat exchange coefficient; μ is viscosity.

Solve for u , v , w and we will calculate the temperature at the time of velocity determination. Converting the whole value from the real coordinate system to the dimensionless coordinate system (Figure 4) and instead of the general equation (1) we get the temperature value T

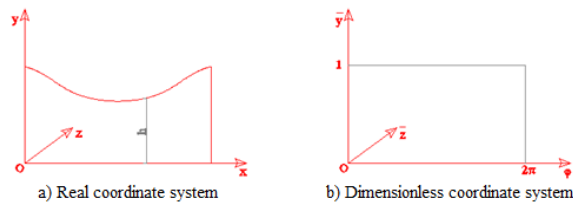


Fig. 4. Converting the real coordinate system to the dimensionless coordinate system

Apply the temperature-dependent viscosity equation (2) to solve the viscosity at the time of determination:

$$\mu = \mu_0 \cdot e^{K \cdot (T - T_0)} \quad (2)$$

Combining the boundary condition. On the contiguous surface between the oil film and the bearing:

$$\frac{\partial T}{\partial y} \Big|_{f-b} = - \frac{k_b C}{k(\theta, z) R} \bar{h} \frac{\partial \bar{T}_b}{\partial \bar{r}_b} \Big|_{f-b} \quad (3)$$

On the contiguous surface between the oil film and the crankshaft:

$$\frac{\partial T}{\partial y} \Big|_{f-s} = 0 \quad (4)$$

At the drain supplying lubricant:

$$\bar{T} \Big|_{f-i} = \bar{T}_{mix} \quad (5)$$

Outside of the bearing:

$$\frac{\partial \bar{T}_b}{\partial \bar{r}} \Big|_{\bar{r}=R_n} = - \frac{h_b R}{k_p} (\bar{T}_b \Big|_{\bar{r}=R_n} - \bar{T}_\alpha) \quad (6)$$

At the two sides of the bearing:

$$\frac{\partial \bar{T}_b}{\partial z} \Big|_{z=0 \text{ or } 1} = - \frac{h_b R}{k_b} (\bar{T}_b \Big|_{z=0 \text{ or } 1} - \bar{T}_\alpha) \quad (7)$$

The integral domain of the oil film is divided into 8-node rectangular elements with Ni interpolation functions written in the natural coordinate system. Conversion from real coordinate system to natural coordinate system (Figure 5) applying finite element model with lubricant film temperature field equation:

$$(K + K_1) \{T_i\} = f \quad (8)$$

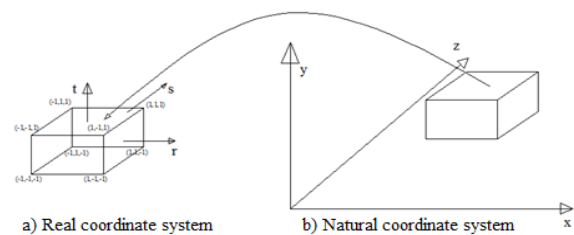


Fig. 5. Conversion from real coordinate system to natural coordinate system

4. Comparison results

The theoretical oil film temperature field is the result of simulating the temperature difference associated with the temperature increase when the connecting-rod big end bearing is operating stably and the oil temperature is supplied. Comparing experimental results with simulation results lubrication oil Besil F100.

The calculation program simulates the

temperature programmed by the Fortran software following the temperature field algorithm as Figure 6.

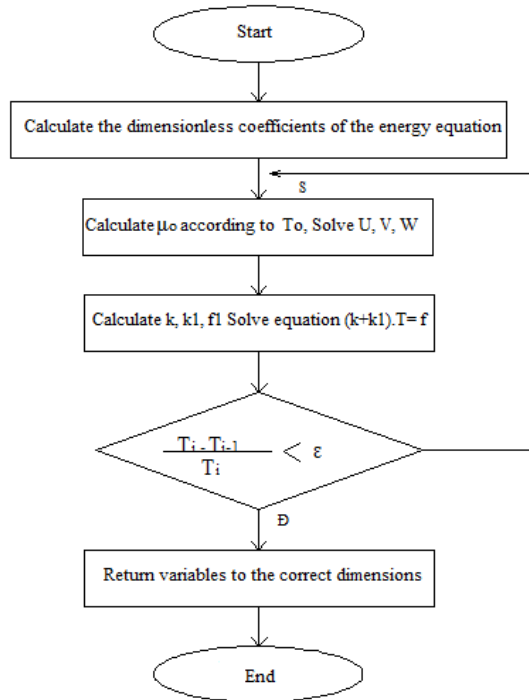


Fig. 6. Temperature field algorithm

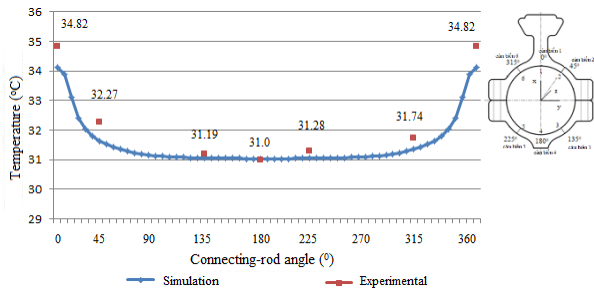


Fig. 7. Comparison of simulation and experimental results of oil film temperature at 100 rpm, 360° angle of crankshaft, Besil F100 lubricating oil.

Figure 7 compares the simulation and experimental results of the diaphragm oil film temperature at the connecting-rod big end bearing speed of 100 rpm with Besil F100 lubricating oil when the connecting-rod big end bearing reaches a steady state after 2500 cycles and the temperature reaches a steady state compared to the inlet temperature. We see simulated oil film temperature and experimental oil film temperature similar in form, however, there is a difference in temperature values at the angles of the connecting rod. Maximum difference of oil film temperature at angles of 0°, 45° and 315° of connecting rod, 34.11°C (calculated result) and 34.82°C (experimental result) at angle 0° of connecting rod, 31.6°C (result calculation) and 32.7°C (experimental result) at angle 45° of

connecting rod, 31.34°C (calculation result) and 31.74°C (experimental result) at angle of 315° of connecting rod. At angle of 180° of the transmission bar, there is almost no difference. At the 225° angle of the connecting rod, the difference is not large, 31.04°C (calculated results) and 31.28°C (experimental results). Large differences are difficult to fully explain but can be explained by the numerical simulation program not including the lubrication effects and also due to measurement errors.

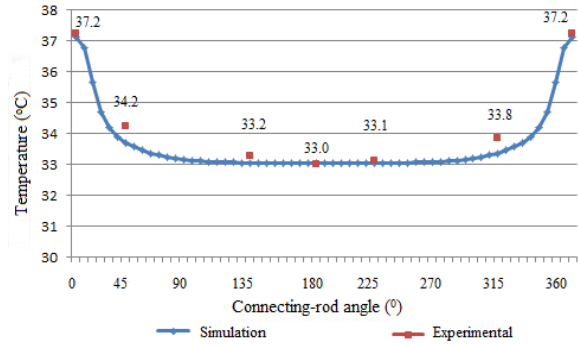


Fig. 8. Comparison of simulation and experimental results of oil film temperature at 150rpm, angle 360° of crankshaft, Besil F100 lubricating oil.

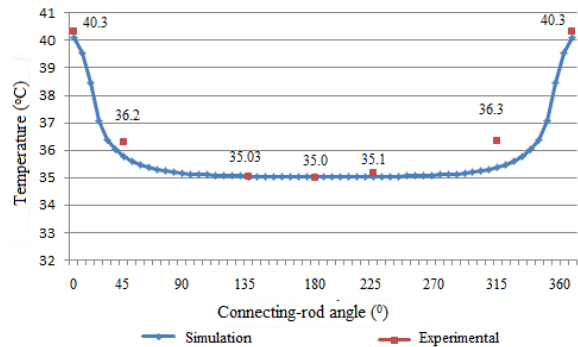


Fig. 9. Comparison of simulation and experimental results of oil film temperature at 200 rpm, angle 360° of crankshaft, Besil F100 lubricating oil.

Figures 8 and figure 9 show simulations and experimental results of the oil film temperature field (temperature difference) at speeds of 150 rpm and 200 rpm with Besil F100 oil. We see that when the speed of rotation increases, the difference between the calculated temperature and the experimental temperature decreases except at the 315° angle of the connecting rod, the deviation increases. In particular, at the angle 0° of the connecting rod, this discrepancy is significantly reduced (37.12°C is the calculated result and 37.22°C is the experimental result), this decrease is due to the increased calculation result. This may explain that the oil film temperature in the maximum load area is mainly influenced by the applied load. At the 315° of the connecting rod, the bias increases. In particular, at the angle 0° of the

transmission, this discrepancy is significantly reduced (37.12° is the calculated result and 37.22°C is the experimental result), this decrease is due to the increased calculation results. This may explain that the oil film temperature in the maximum load area is mainly influenced by the applied load. At the 3150 angle of the connecting rod, the experimental temperature increased to 33.8°C, the calculated simulation temperature was 33.04°C. Thus, the big difference between experimental results and calculated results is due to the increase in experimental temperature.

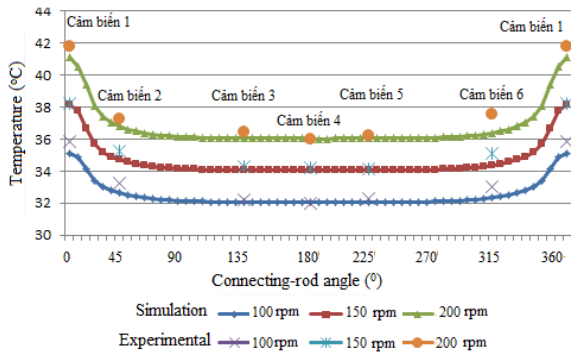


Fig. 10. Comparison of simulation results and experimental temperature of oil film at different speeds, angle 360° of the crankshaft, Atox 320 lubricating oil when the connecting-rod big end bearing reaches a steady state

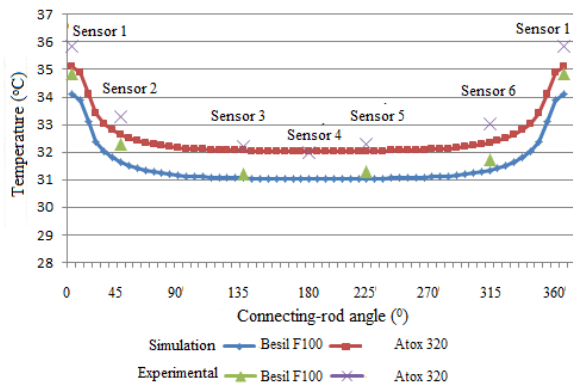


Fig. 11. Comparison of simulation and experimental results of oil film field temperature at the angle of 360° crankshaft at 100 rpm with Besil F100 oil and Atox 320 oil

Similar to Besil F100 oil, when lubricated with Atox 320 oil, the temperature of the oil film is the same rule as the difference between simulation and experimental results (Figure 10). The oil film temperature results are determined when the drive has worked stably. With the speed of 100 rpm, 150 rpm and 200 rpm, the drive is stable operation after 1500, 2000, 2500 cycles. At the lowest speed (100 rpm), the biggest differences are at the positions 0°, 45° and 315° of the transmission. When the rotation speed is

higher, at 150 rpm and 200 rpm, the calculated and experimental oil film temperature difference decreases, except at the 315° angle of the transmission, the difference is increased.

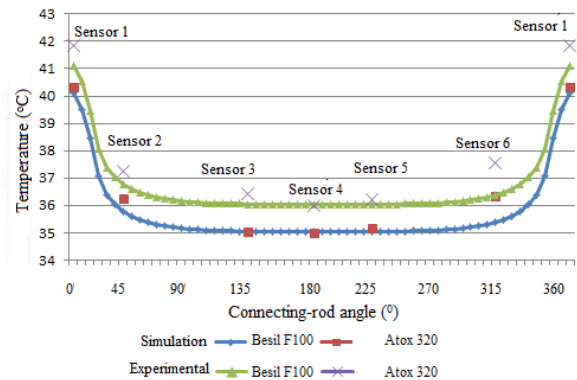


Fig. 12. Comparison of simulation and experimental results of oil film temperature field at the angle of 360° crankshaft at 200 rpm with Besil F100 oil and Atox 320 oil.

Figure 11 compares the simulation and experimental results of the oil film temperature field at 100 rpm with Atox 320 and Besil F100 oils. Figure 12 compares the simulation and experimental results of oil film temperature field at 200 rpm with Atox 320 and Besil F100 oils. Both comparisons have similar results between theory and experiment, but at the 315° angular position of the connecting rod, the higher the speed, the higher the temperature difference between theory and experiment. Although the difference is less than 10° C, there is a difference when the speed of rotation is increased due to the high speed on the heat transfer and heat exchange of experiment between the angle 0° and the angle 315° is slightly slower. Therefore, the experimental temperature is higher than the theory at the 315° angular position of the connecting rod at high speed. The experimental results are higher than the theoretical results, but the difference is not significant in all comparison cases. There is a higher difference of the experimental results than the theoretical results due to the experimental error, but the difference is only 0.2°C to 0.5°C, the graphical characteristic lines still coincide with each other.

From the simulation results and experimental results, we see that the temperature field of the lubricating oil film in the large end of the transmission rod has similar temperature characteristics. As the rotation speed increases, the temperature increase also increases, the faster the rotation speed is, the higher the temperature increases. Maximum temperature value is at the angle 0° (360°) of the connecting rod. Lowest temperature value is at the angled 180° position of the connecting rod.

5. Conclusion

The temperature field of simulated oil film and experimental oil film temperature are similar in form, but there is a difference in value. When the drive is stable, at the angle of 0° , 45° and 315° of the connecting rod, the difference between the calculated and experimental results is the highest, 34.11°C (calculated results) and 34.82°C (experimental results) at angle 0° of the connecting rod, 31.6°C (calculated results) and 32.7°C (experimental results) at 45° of the connecting rod, 31.34°C (calculated results) and 31.74°C (experimental results) at 135° of the connecting rod. At the 180° angle of the connecting rod, there is almost no difference. At the 225° angle of the connecting rod, the difference is not large, 31.04°C (calculated results) and 31.28°C (experimental results). These differences are difficult to fully explain but can be explained by the numerical simulation program not including the lubrication effects and also due to errors in measurement. At low speed (100 rpm), the maximum difference between the simulated oil film temperature and the experimental temperature at 0° , 45° and 315° positions of the connecting rod. But when the rotation speed is higher (150 rpm / 200 rpm), the temperature difference decreases, except at the 315° angle of the transmission the difference increases. The difference in temperature increases due to an increase in the experimental temperature. The principle of this difference in temperature is the same for Besil F100 and Atox 320 lubricants. This can be explained by the fact that when the rotation speed increases, the heat transfer and heat exchange of the experiment between the angular position 0° and 315° are quite slower. The experimental results are higher than the theoretical results, but the difference is not significant in all comparison cases. There is a higher difference of the experimental results than the theoretical results due to the experimental error, but the difference is only 0.2°C to 0.5°C . The temperature of the oil film in the connecting-rod big end bearing increases when the rotation speed increases and reaches the maximum value at the middle section of 360° angle of the crankshaft when there is an explosion. The higher viscosity the lubrication oil has, the higher

temperature of the oil film is in the connecting-rod big end bearing.

References

- [1] Reddi, M.M, 1969, Finite Element Solution of the Incompressible Lubrication problem. ASME, Journal of Lubrication Technology, pp.262 – 270.
- [2] Oh, K.P., Huebner, K.H., 1973, Solution of the Elastohydrodynamic Finite Journal Bearing Problem. ASME Journal of Lubrication Technology, Vol. 3, pp.342 – 352.
- [3] H. Shahmohamadi , R. Rahmani, H. Rahnejat , C. P. Garner , D. Dowson(2015), Big End Bearing Losses with Thermal Cavitation Flow Under Cylinder Deactivation. Tribol Lett (2015) 57:2.
- [4] N. Morris, M. Mohammadpour, R. Rahmani, P.M. Johns-Rahnejat, H. Rahnejat1 and D. Dowson (2018), Effect of Cylinder Deactivation on tribological performance of piston compression ring and connecting-rod bearing.”, Tribology International (2018), doi: 10.1016/j.triboint.2017.12.045..
- [5] Piere-Eugene J.(1983), Contribution à l’Etude de la Déformation Elastique d’un Coussinet de Tête de Bielle en Fonctionnement Hydrodynamique Permanent, Thèse de Doctorat de l’Université de Poitiers..
- [6] Moreau H.(2001), Mesures des Epaisseurs du Film d’Huile dans les Paliers de Moteur Automobile et Comparaisons avec les Résultats Théoriques, Thèse de Doctorat de Université de Poitiers
- [7] Michaud P(2004), Modélisation thermo élasto hydro dynamique tridimensionnelle des paliers de moteurs. Mise en place d'un banc d'essais pour paliers sous conditions sévères", Thèse de Doctorat à Université de Poitiers.
- [8] Fatu A.(2005), Modélisation numérique et expérimentale de la lubrification de palier de moteur soumis à des conditions sévères de fonctionnement”, Thèse de doctorat de l’Université de Poitiers.
- [9] M’hammed El Gadari ,n, Aurelian Fatu ,, Mohamed Hajjam.(2016), Shaft roughness effect on elasto-hydrodynamic lubrication of rotary lip seals: Experimentation and numerical simulation", journal homepage: www.elsevier.com/locate/triboint